DOI til publisert versjon / DOI to published version: 10.1109/TGRS.2014.2346473

Temporal Stability of X-Band Single-Pass InSAR Heights in a Spruce Forest: Effects of Acquisition Properties and Season

Svein Solberg, *Member, IEEE*, Dan Johan Weydahl, and Rasmus Astrup

***Abstract*—We investigated the stability of TanDEM-X interferometric synthetic aperture radar (InSAR) heights across eight repeated acquisitions. With InSAR height we mean the height above ground of the scattering phase center. We obtained InSAR heights by subtracting a digital terrain model generated from airborne laser scanning. The acquisitions varied in polarization, normal baseline, and season. The study area was a spruce forest in southeastern Norway. We established 179 field plots within 26 selected forest stands and obtained aboveground biomass (AGB) from field inventory. The InSAR heights were generally stable across the acquisitions as was the relationship between AGB and InSAR height, although systematic and random variations were noted. Two acquisitions had close-to-identical technical properties and weather conditions, and they produced close-to-identical InSAR heights. InSAR heights were fairly stable across a range in temperature and precipitation through spring, summer, and autumn, across a range in baseline values and for both HH and VV polarizations. However, a winter acquisition at temperatures of −7 °C had much deeper penetration into the canopy and generated considerably lower InSAR heights and, hence, a very different relationship with biomass. Higher random errors were noted in a cross-pol data set due to lower backscatter and when the normal baseline was very small or very large. A height of ambiguity around 20–50 m appeared to be optimal. Interferometric X-band SAR can be used for monitoring coniferous boreal forests as long as the season and technical properties of the acquisition are kept within certain ranges.**

***Index Terms*—Acquisition properties, forest biomass, forest monitoring, interferometric synthetic aperture radar (InSAR), single pass, synthetic aperture radar (SAR), temporal changes, X-band.**

I. Introduction

SATELLITE remote sensing with interferometric synthetic aperture radar (InSAR) and radargrammetry has a potential for forest monitoring due to their ability to provide digital surface models (DSMs). The height above ground of the DSM is largely determined by vegetation height and vegetation density, and these two properties are also largely determining biomass and volume [1]. The advantage of this in comparison with other remote sensing methods is that biomass and volume can be estimated if a digital terrain model (DTM) is available [2]; temporal changes from growth and logging are detectable without a DTM [3]; in addition, SAR does not suffer from cloud problems.

However, a key question remains to be clarified before this can be developed into an operational method. How stable is the relationship between a SAR height and forest biomass, and how similar must the properties of repeated acquisitions in a monitoring scheme be?

The SAR microwaves penetrate into vegetation, and the penetration depth is determined by technical properties of the acquisition and by climatic factors. For forest monitoring applications, it is crucial to understand how similar the technical properties must be and how similar the climatic conditions must be. The penetration increases with wavelength and is smaller for X-band compared with C-, L-, and P-bands. Hence, in general, the SAR wavelength needs to be fixed, although the difference in penetration depth between X- and C-bands is but a few meters [4], and it has been demonstrated that logging can be detected as a decrease from a C-band Shuttle Radar Topography Mission (SRTM) DSM in 2000 to an X-band COSMO-SkyMed or TanDEM-X DSM in 2012 [3], [5]. A copolarized acquisition might penetrate deeper than a cross-polarized one, because the backscatter contribution from the ground is higher in the former, whereas the backscatter contribution from foliage and branches is larger in the latter. The normal baseline of the interferometric radar antenna may also affect the derived penetration depth. The baseline influences the uncertainty of the derived elevations by influencing the decorrelation of the interferometric signal and the height ambiguities. The extinction of the microwaves through a canopy volume varies with the dielectric constant, and deeper penetration will be the case in dry or frozen vegetation [6], [7]. In this paper, we apply X-band InSAR data from the bistatic (or single-pass) acquisitions of the TanDEM-X mission, focusing on InSAR height, i.e., the height above ground of the scattering phase center. The aims of this study were as follows:

1) to describe how stable InSAR heights and their relationship with biomass in a forest are;
2) to identify the main causes of the variation.

II. Materials and Methods

A. Study Area

This study was carried out in Lardal municipality in southeast Norway and was centered at 59.4° north and 9.9° east. The study area is dominated by coniferous forest with intermixed

Manuscript received September 30, 2013; revised January 15, 2014 and June 25, 2014; accepted August 1, 2014. This work was supported in part by the European Space Agency through the PRODEX fund and in part by the Norwegian Forest and Landscape Institute.

S. Solberg and R. Astrup are with the National Forest Inventory, Norwegian Forest and Landscape Institute, 1431 Ås, Norway.

D. J. Weydahl is with the Division for Electronics, Norwegian Defence Research Establishment, 2027 Kjeller, Norway.

Digital Object Identifier 10.1109/TGRS.2014.2346473

DOI til publisert versjon / DOI to published version: 10.1109/TGRS.2014.2346473

peat lands and lakes and a valley with agricultural lands. The forest is managed for timber production and contains stands of various age and development stages. A digitized forest stand map was available for this study.

B. Field Data

In 26 spruce-dominated stands, we randomly selected seven locations for field plots. Three plot locations were discarded, because they were located in a part of the stand that has been clear cut recently, leaving 179 field plots for this study. The locations of the plot centers were accurately recorded with differential geographic positioning system measurements. The plots were circular and is 250 m^2. On the plots, we carried out field inventory in accordance with the methods used on the Norwegian National Forest Inventory [8]. Species and diameter at breast height were recorded for all trees above 5 cm at breast height. Tree height was measured for a subset of ten trees per plot, and the heights of the remaining trees were estimated based on diameter–height relationships derived for each plot. Aboveground biomass (AGB) was derived for all trees with species-specific allometric models for the biomass components stem wood, stem bark, stump, and live and dead branches [9]. AGB varied from 0 to 338 t/ha, with a mean value of 135 t/ha.

C. ALS Data

The study area was covered by airborne laser scanning (ALS) in May 2009 by the commercial company BLOM Geomatics, with a PA31 Piper Navajo aircraft flying at 690-m elevation. The utilized sensors were Optech ALTM05SEN180 and ALTM04SEN161 with a pulse repetition frequency of 125 kHz, which produced a data set of 10 pulses/m^2. From the operator, we obtained both the point cloud and the terrain points, from which we generated a DTM and the 90 percentile height above ground values of the first echoes (P90), both having 10 m $\times$ 10 m spatial resolution.

D. TanDEM-X Data

We established a data set of eight TanDEM-X acquisitions. The overlap of these acquisitions made up the 426-km^2 study area. The acquisitions are listed in Table I, showing the variety of properties that made this data set a good fit for the aim of this study. Acquisitions 1–5 were similar by all having HH-HH polarization and ascending orbit, whereas they differed concerning the normal baseline and the season (see Table I). The last three acquisitions (6–8, Table I) had a descending orbit and a small baseline. The polarizations were HH-HH and VV-VV from single-pol acquisitions (1–7, Table I), and one cross-pol HV-HV from a dual-pol acquisition (8). The acquisitions were done during July 13, 2011 to February 14, 2013. The incidence angles varied from 36° to 45°. The data were received as coregistered single-look complex data in CoSSC format. The pixel spacing in the CoSSC data varied from 0.9 to 1.4 m in range and from 1.9 to 2.2 m in azimuth. The SAR antenna normal baselines varied from 13 to 429 m, which were all well below the critical baseline of 3600 m. The height of ambiguity (HoA), which is the height difference corresponding to a complete 2π cycle of the interferometric phase, is related to the normal baseline, as noted by [10]

TABLE I
KEY PROPERTIES OF THE TANDEM-X ACQUISITIONS: DATE, ORBIT DIRECTION, POLARIZATION, INCIDENCE ANGLE (θ_i), NORMAL BASELINE ($B_\perp$), AND HOA

Acquisition	Date	Orbit	Polarization	θ_I, degrees	$B_\perp$, m	HoA, m
1	23.07.2011	ascending	HH-HH	36	251	23
2	05.09.2011	ascending	HH-HH	36	238	24
3	15.05.2012	ascending	HH-HH	36	429	13
4	03.07.2012	ascending	HH-HH	45	426	18
5	14.02.2013	ascending	HH-HH	36	233	25
6	01.09.2011	descending	HH-HH	43	59	122
7	24.07.2011	descending	VV-VV	34	17	316
8	13.07.2011	descending	HV-HV*	34	13	393

* Taken from a dual-pol acquisition

$$\text{HoA} = \lambda r \sin(\theta_i)/B_\perp \tag{1}$$

where λ is the radar wavelength, r is the slant range, θ_i is the incidence angle, and $B_\perp$ is the normal baseline.

Each image pair was processed to an InSAR DSM using the Sarscape 5.0 module of the ENVI 5.0 software as follows: An interferogram was generated from each image pair and was further processed into a differential interferogram by removing the range-dependent and terrain-topography-dependent parts of the phase differences by using the ALS DTM as input. These differential interferograms represented the phase differences caused by vegetation height in addition to phase noise and possible inaccuracies in the orbit data or in the atmospheric corrections. The phase noise in the TanDEM-X data could result from volume decorrelation and system noise. The differential interferograms were filtered with the Goldstein filter [11], which reduces phase noise and enables an accurate phase unwrapping later. We applied the default settings of the Goldstein filter. We removed phase offset and phase ramp errors originating from possible orbit and atmospheric inaccuracies by fitting the following model to 66 ground control points (GCPs) commonly used for all TanDEM-X pairs:

$$\Delta\varphi = k_0 + k_1\text{RG} + k_2\text{AZ} \tag{2}$$

where $\Delta\varphi$ was the phase difference at each GCP; k_0, k_1, and k_2 were correction factors; and RG and AZ were the range and azimuth coordinates, respectively. The GCPs were subjectively laid out at locations without trees, i.e., where the InSAR DSM should have the same elevation as the DTM. These locations

DOI til publisert versjon / DOI to published version: 10.1109/TGRS.2014.2346473

TABLE II
OFFSET (IN MIDDLE OF IMAGE) AND RAMP CORRECTIONS (m PER 10 km) AND RESIDUAL HEIGHT ERROR (RMSE) OF THE 66 GCPs AFTER CORRECTION

Acquisition	Mean offset	10 km ramp EW	10 km ramp SN	RMSE
1	-1.3	0.0	0.7	1.3
2	-7.4	-2.1	-0.4	1.2
3	-3.4	-1.3	0.4	1.1
4	1.4	-0.3	-0.7	1.1
5	5.3	2.6	1.9	1.1
6	-8.5	-8.2	7.6	1.6
7	33.3	-29.6	8.1	2.7
8	43.2	-37.8	12.4	3.7

were selected as having high coherence and relatively flat terrain with low fringe density, i.e., in clear cuts and agricultural fields. In order to identify suitable GCP locations, the coherence files of the eight acquisitions were geocoded and overlaid, as were a number of the filtered differential interferograms. The offset corrections in X- and Y-directions varied considerably from a few to 43 m (see Table II). In addition, the ramp corrections (in the Z-direction) varied considerably. For the ascending acquisitions (1–5), there were almost no ramp errors. However, for the descending acquisitions (6–8), they were considerable both in range and azimuth directions. Over a 10-km distance, they were between 8 and 38 m. After removing the offset and ramp errors, the height errors in the GCPs were mostly minor, varying from 1.1 to 3.7 m (see Table II). This is well below what was found in the X-band SRTM data in the same part of Norway by [4], who did not use ramp corrections.

We carried out phase unwrapping using the minimum cost flow method. Some of the acquisitions had an HoA value higher than the tree heights, and we could have cancelled the unwrapping and converted phase values directly to InSAR heights. However, it was carried out in order to have one and the same processing chain for all acquisitions. Finally, the unwrapped phases were converted into elevation data and transformed from satellite slant-range geometry to geocoded DSMs. During the processing, we used a multilooking varying from 4 to 6 in range and from 4 to 5 in azimuth, which corresponded to about 10 m $\times$ 10 m. This was also the spatial resolution of the geocoded DSMs obtained by fourth-order cubic convolution resampling. We subtracted the DTM from the DSM and obtained InSAR heights.

We calculated backscatter intensity (σ^0). The intensity data were calibrated and normalized taking the following into account: 1) the illuminated area of each resolution cell based on the topography from the ALS DTM and the incidence angle; 2) the variations in antenna gain using the ALS DTM; and 3) the distance variation from the near range to the far range (range spread loss).

E. Analyses

We averaged the biomass and InSAR height data for each stand, resulting in a data set with 26 observations, i.e., 26 stands. We assumed no biomass change during the 19-month study period, as the annual growth in this spruce forest is small with a forest rotation period of about 80 years and because no logging was carried out in the selected stands. We fitted a no-intercept regression model to the data, in line with findings in the same study area [2], using ordinary least squares, i.e.,

$$\text{AGB} = \beta H + e \tag{3}$$

where β was a slope parameter, H was the InSAR height, and e was the residual error. A curvilinear relationship might be expected, because the relationship between a stem volume and a tree height variable, i.e., mean tree height or top height, has been found to be curvilinear [12]–[14]. However, we chose model (3) because no tendency of curve linearity has been found for the relationship between biomass and InSAR height in this forest type [2]. In addition, by excluding an intercept, the model should be physically correct by having the center of the backscatter at the ground in a clear cut, and this way, we also avoided the problem with inflated intercepts and underestimated slopes, which is common in regression models based on data sets having measurement errors on the explanatory variable [15]. We calculated the coefficient of determination as recommended by [16] for no-intercept models, i.e.,

$$R^2 = 1 - \frac{n}{n-p} \frac{\sum (y-\hat{y})^2}{\sum (y-\hat{y})^2} \tag{4}$$

where n was the number of observations (26 stands), p was the number of model parameters (1), y was the field measured biomass, $\hat{y}$ was the modeled biomass, and $\bar{y}$ was the mean of all observations y, and the residual error as

$$\text{RMSE} = \left[n^{-1} \sum (\hat{y} - y)^2 \right]^{0.5}. \tag{5}$$

In order to estimate the accuracy both at the plot and stand levels, we fitted an alternative model to (3) with a hierarchical random effects structure, i.e., plots within stands, to the complete data set with the 179 plots, i.e.,

$$\text{AGB} = \beta H + s + e \tag{6}$$

where s and e were zero-mean Gaussian variables representing the random effects at the stand and plot levels, respectively. We applied the MIXED procedure in the SAS software [17].

III. RESULTS AND DISCUSSION

For most of the acquisitions, the InSAR heights and their corresponding relationships with biomass were relatively stable. The noise and errors in the relationship were also relatively stable; however, with some clear exceptions.

DOI til publisert versjon / DOI to published version: 10.1109/TGRS.2014.2346473

TABLE III
MEAN VALUES AND RANGES OF INSAR HEIGHT FOR THE 179 FIELD PLOTS

Acquisition	mean	std	min	max
1	9.4 m	3.9	-0.1	19.5
2	9.3 m	3.8	-0.1	17.4
3	8.8 m	4.9	-4.9	22.0
4	10.9 m	4.4	0.1	20.6
5	5.4 m	2.4	-0.8	12.6
6	10.0 m	4.1	1.6	22.6
7	9.5 m	4.3	-0.5	20.3
8	8.6 m	5.4	-1.9	25.9

TABLE IV
PEARSON CORRELATION MATRIX FOR THE INSAR HEIGHTS, $n = 179$

Acquisition	1	2	3	4	5	6	7	8
1	1.00	0.99	0.68	0.98	0.87	0.88	0.83	0.64
2	0.99	1.00	0.72	0.98	0.88	0.87	0.83	0.63
3	0.68	0.72	1.00	0.67	0.69	0.53	0.52	0.28
4	0.98	0.98	0.67	1.00	0.85	0.88	0.84	0.65
5	0.87	0.88	0.69	0.85	1.00	0.74	0.70	0.52
6	0.88	0.87	0.53	0.88	0.74	1.00	0.88	0.77
7	0.83	0.83	0.52	0.84	0.70	0.88	1.00	0.66
8	0.64	0.63	0.28	0.65	0.52	0.77	0.66	1.00
avg	0.86	0.86	0.64	0.85	0.78	0.82	0.78	0.64

A. InSAR Height Statistics

The InSAR heights were relatively stable. The majority of acquisitions had similar mean values and standard deviations (see Table III). In seven of eight cases (all except acquisition 5), the mean value was between 8.6 and 10.9 m. Five of these had similar mean values, around 9 m, and similar ranges, from about 0 to 20 m. However, some deviations were also present. Acquisitions 3 and 8 had wider height ranges, with minimum values below zero, which indicates more noisy results. Acquisition 5 strongly deviated from the others. The mean value was considerably lower, i.e., 5 m, with a corresponding narrow range from -1 to 13 m.

The stability of the InSAR heights was also evident as they varied consistently over the study area. The InSAR heights of the acquisitions were correlated with each other (see Table IV). On average, the Pearson correlation coefficient was 0.8, and it varied from 0.28 to 0.99. Overall, acquisitions 3 and 8 had weakest correlations, with an $r = 0.64$, which again indicated more noise in these.

B. Biomass Models

In line with the temporal stability seen in InSAR heights, their relationships with biomass also remained fairly stable. With one exception (acquisition 5), the slope estimate β was relatively stable among the acquisitions—varying from 13.6 to 14.8 t/ha/m (see Fig. 1). This indicates that AGB changed with

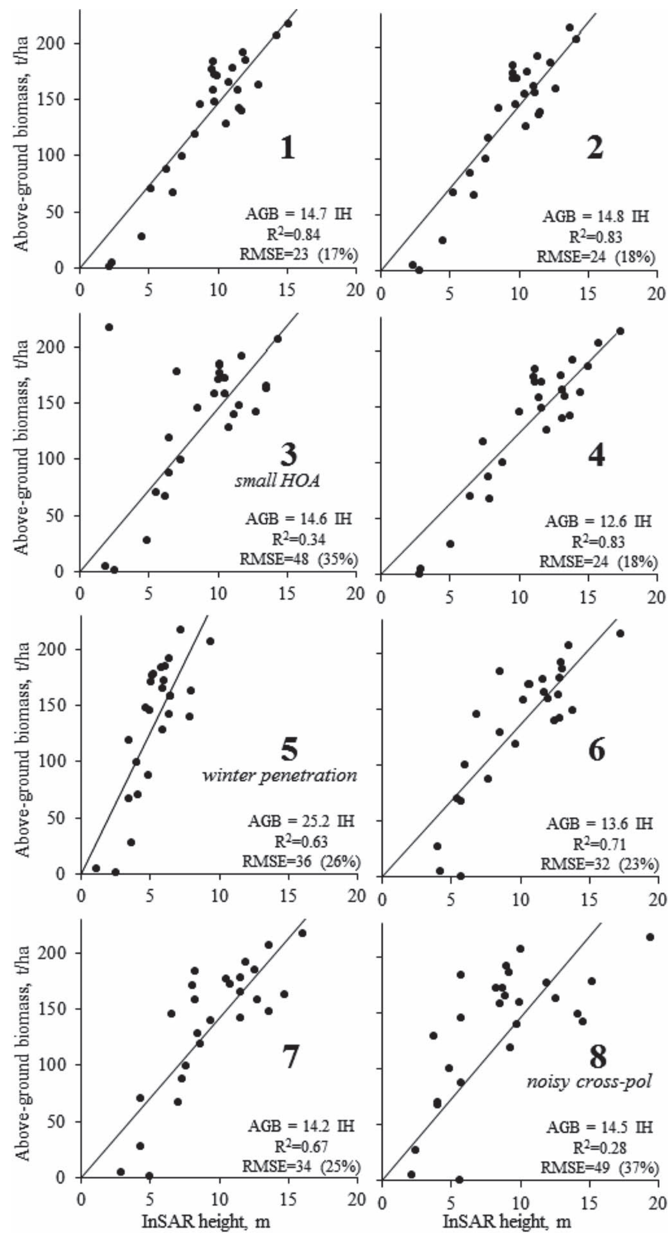

Fig. 1. AGB plotted against InSAR height for the eight acquisitions. The data points are stand means, i.e., mean values of seven field plots within each stand. No-intercept regression models are fitted to the data. Acquisition 3 had one clear outlier in the upper left corner due to problems with small HoA (see below), acquisition 5 had deep canopy penetration apparently due to frozen conditions (see below), and acquisition 8 was generally noisy, which is related to a lower signal-to-noise ratio (see below).

about 14 t/ha/m change in InSAR height. Acquisition 5 deviated considerably from the other acquisitions, with a slope of 25.2 t/ha/m.

There was no evident curve linearity, or saturation, in the relationships. The straight regression line through the origin followed the data closely, except for the 2–3 stands with the lowermost biomass values. For these stands, with biomass close to zero, one might expect the center of the backscatter to be at, or just above, the ground. However, these stands had InSAR heights from 2 to 5 m above ground.

The residual error in (3) varied between the acquisitions from 17% to 26% of mean biomass (acquisitions 1, 2, 4, 5, 6, and 7)

DOI til publisert versjon / DOI to published version: 10.1109/TGRS.2014.2346473

TABLE V
BACKSCATTER COEFFICIENT σ^0 FOR THE ACQUISITIONS

Acquisition	Mean	Minimum	Maximum
1	0.15	0.01	0.56
2	0.13	0.01	0.51
3	0.11	0.02	0.35
4	0.09	0.01	0.27
5	0.17	0.02	0.62
6	0.12	0.01	0.67
7	0.17	0.01	0.98
8	0.03	0.01	0.12

and from 35% to 37% in acquisitions 3 and 8. It can be noted that there was one clear outlier in the upper left corner of scatterplot 3, which will be discussed in the following in relation to the normal baseline and HoA. In comparison, a similar modeling was carried out with the ALS variable P90. The slope was slightly lower (11.0 t/ha/m), and the model was somewhat more accurate, with $R^2 = 0.89$ and a residual error of 19.3 t/ha (14.3%).

With the hierarchical random effect model (6), the estimated random error at the stand level was somewhat lower than that obtained from model (3), varying from 11.5 to 70.1 t/ha. Acquisitions 1, 2, and 4 had the lowest RMSE values of 11–14 t/ha/m, which corresponded to 9%–10% of the mean biomass (135 t/ha). Acquisitions 5, 6, and 7 had slightly higher errors (24–32 t/ha, 18%–24%), whereas acquisitions 3 and 8 had the highest errors (55–70 t/ha, 41%–52%). At the plot level, the errors were fairly similar for all acquisitions, varying from 52 to 61 t/ha, which corresponded to 38%–43% of mean biomass.

C. Causal Factor 1: Polarization

Acquisition 8 appeared to be particularly noisy, as noted above. This acquisition also had a number of other indicators of poor performance. It had the largest offset and ramp errors (see Table II). On average, the offset was 43 m, while the ramp corrections were −38 m in the east-west direction and 12 m in north-south. The InSAR heights had a wider range, including negative values down to −1.9 m and unrealistically high values up to 25.9 m (see Table III). This was the acquisition with the InSAR heights most weakly correlated to the other acquisitions (see Table IV). It provided the least accurate biomass model, with an RMSE of 52% at the stand level (see Fig. 1). This was a cross-pol HV-HV data set taken from a dual-pol acquisition. The more noisy results can be attributed to a lower signal-to-noise ratio. The backscatter values were markedly lower than in the other acquisitions (see Table V), which is typical for cross-polarized data.

D. Causal Factor 2: Normal Baseline

The normal baseline, which is closely related to the coherence and noise level, as well as to HoA, had major impacts on the results. The most accurate biomass estimates were obtained with normal baseline values in the range 230–420 m. This corresponded to HoA values around 20 m, while the errors increased with smaller and larger HoA values. Acquisitions 1, 2, and 4 had HoA values from 18 to 24 m, and the stand level errors of their biomass models were lowest with 23–24 t/ha (17%–18% of mean biomass) (see Fig. 1). These three acquisitions also had only minor offset and ramp corrections (see Table II), as well as the highest InSAR height correlations (see Table IV). Acquisition 3 had a large biomass model error, which likely is caused by a HoA value of only 13.4 m, which is well below the maximum InSAR heights. Acquisitions 6 and 7 had a slightly higher biomass model error, higher offset and ramp corrections, and slightly lower InSAR height correlations. Acquisitions 5 and 8 had higher errors; however, there were other likely causes for that: Acquisition 5 was taken under winter conditions (see below), and acquisition 8 was noisy due to the HV-HV polarization (see above).

The results with an optimum HoA value around 20 m indicate that there are different types of errors present and that these error types vary with HoA. First, there is one type of error that increases with HoA. If we consider that the SAR hardware system has a certain range of quantization levels, or byte depth, this will correspond to a certain span or resolution in phase values, or minimum distinguishable phase differences (i.e., quantization levels). If the HoA is large, such a minimum distinguishable phase difference will correspond to a large height difference. This increase in relative height error ($\Delta h_{90\%}$) with increasing HoA is noted by [10]

$$\Delta h_{90\%} = \text{HoA} \cdot \Delta\varphi_{90\%}/2\pi \qquad (7)$$

where $\Delta\varphi_{90\%}$ is the relative, or 90% point-to-point, phase error.

Second, at small HoA values, there are two error types that occur: increasing phase noise and height ambiguities. Small HoA values result from large normal baselines where volume decorrelation occurs in forests. The phase noise will be then considerably higher over a forested area if the baseline is large and the HoA is small. In addition, at small HoA values, problems occur because phase ambiguities are mixed up with phase noise. This might occur when the HoA is smaller than the maximum InSAR height, because pixels close to the ground and pixels somewhere up in the canopy would have the same phase values and ambiguous heights. This would be a particular problem at forest edges and with scattered large trees, e.g., scattered seed trees left after logging. As shown in Table III, the maximum InSAR height was about 20 m. Hence, in our study area, we might expect this type of error to occur with HoA values below 20 m. However, Fig. 2 indicates that the problem occurred only in acquisition 3, where the HoA value was only 13 m. For acquisition 3, this error type clearly occurred in one of the 26 forest stands. This stand shows up as an outlier in the upper left corner of the scatterplot in Fig. 1. The mean InSAR height of this stand was 2.2 m for acquisition 3, while the average InSAR height of the other acquisitions was 15.2 m. A closer look on the differential interferogram in this stand and this acquisition shows how difficult it is to separate real phase height variations from phase noise (see Fig. 3). The Goldstein filter removed both phase noise and real phase heights, which resulted in phase heights close to zero. For comparison, the

DOI til publisert versjon / DOI to published version: 10.1109/TGRS.2014.2346473

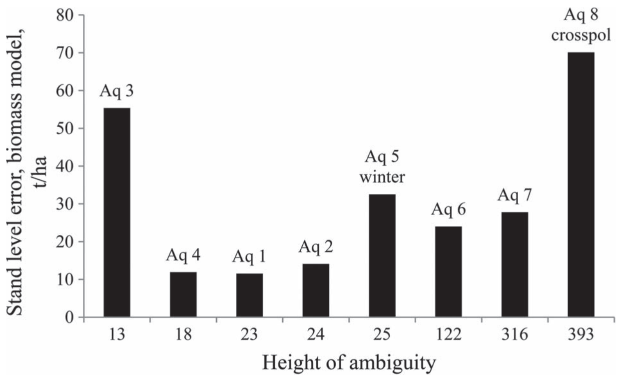

Fig. 2. Stand level errors in the biomass model [6] plotted against HoA.

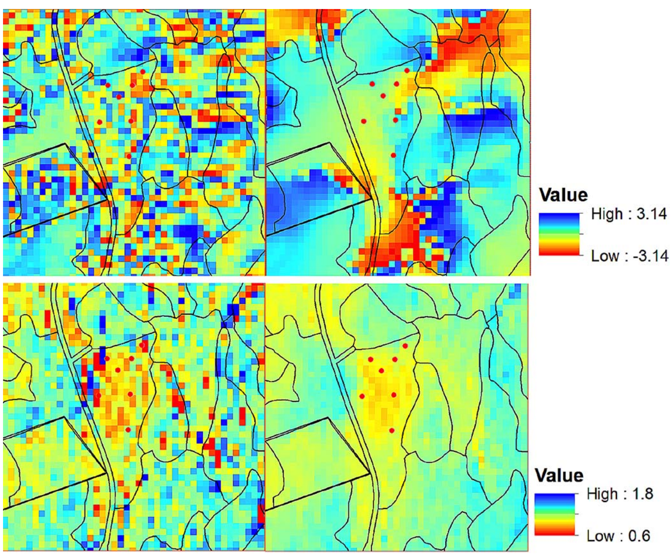

Fig. 3. Part of the InSAR processing chain for a 450 × 450 m large part of the study area centered on the forest stand where acquisition 3 had severe error in InSAR height. Red dots indicate the position of the seven field plots in the stand. (Top) Acquisition 3: (left) differential interferogram; (right) filtered differential interferogram. (Bottom) Acquisition 6: (left) differential interferogram; (right) filtered differential interferogram.

corresponding interferograms are shown for acquisition 6. In this case, the pixels affected by phase noise were more easily identified as a few scattered extreme values. A height profile from west to east through the center of this stand is shown in Fig. 4. As can be seen, at the distance interval from 130 to 250 m, acquisition 3 had InSAR height values of but a few meters, whereas the other acquisitions (except acquisition 5) and the ALS height P90 had heights around 18 m. It needs to be emphasized here that this type of error occurred in only one of the 26 forest stands in acquisition 3. Hence, the Goldstein filter was able to distinguish phase noise from real phase heights in most cases. Thus, the error type was not frequent; however, when present, its magnitude was severe.

Altogether, the optimal HoA for forest monitoring is a tradeoff between the errors increasing with HoA and those decreasing with HoA. For the present forest type, a Norway spruce-dominated forest with maximum tree heights of about 30 m, the optimum HoA would be about 20–50 m. With

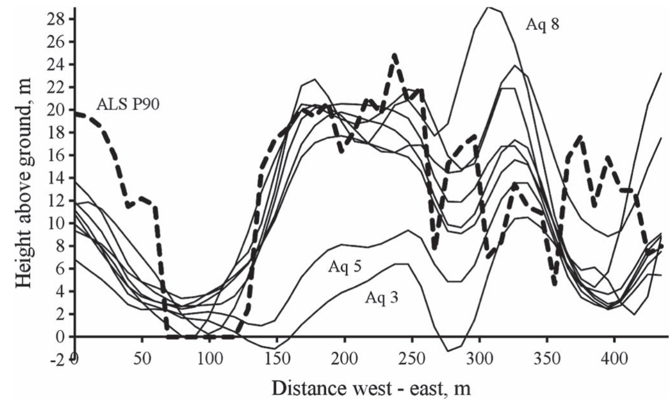

Fig. 4. InSAR heights along a 450-m west–east transect through the center of the area shown in Fig. 3. Three acquisitions (3, 5, 8) having marked deviations from the overall height pattern are labeled. The ALS P90 height is also shown.

these values, we would avoid the confusion between real phase height variations and phase noise, while the baseline is kept low enough to get reasonably high coherence, and finally, the errors related to byte depth, or quantization error, would be kept reasonably low. The TanDEM-X mission is organized with two different acquisition periods: one working with HoA around 50 m and another working with HoA around 35 m. For the present study area, the presented results indicate that both these alternatives should work well. However, for forests with considerably taller trees, the 50-m HoA should be preferred.

Some other properties of the InSAR height data are also evident in Fig. 4. First, the InSAR heights of acquisition 8 were noisy and, for example, contained an unrealistic high value of 29 m at a 300-m transect distance. Second, it is evident that the InSAR DSMs hardly reached down to the ground in treeless area. At the 70- to 120-m transect range, the ALS P90 was down at the ground, clearly showing that no trees were present here. The InSAR heights were mostly around 2–4 m here. To some extent, acquisitions 5 and 6 had zero heights here. This failure of the InSAR DSMs to come down to the ground explains how the zero-biomass plots had a few meters InSAR height, as shown in Fig. 1. However, there were also other challenges in this particular area. The terrain was sloping considerably upward from west to east, with a slope around 25° at 250- to 290-m transect range, and as much as 35° at 320- to 400-m transect range. The steep slope in the latter range generated layover effects in acquisitions 1, 2, 3, and 5. In addition, at 0- to 60-m range, the transect followed an east-west stand boundary separating a clear-cut area to the south from an older spruce stand to the north. While the ALS P90 picked up this boundary sharply with heights varying between 0 and 20 m, the InSAR heights were smoother and showed intermediate heights around 6 m here.

E. Causal Factor 3: Season and Climatic Conditions

Some of the results could be attributed to season or climatic conditions. In general, the acquisitions had fairly similar InSAR heights, except acquisition 5 (see Table III and Fig. 1). Acquisi-

DOI til publisert versjon / DOI to published version: 10.1109/TGRS.2014.2346473

TABLE VI
METEOROLOGICAL DATA FOR THE TANDEM-X STUDY AREA IN NORWAY, SORTED BY DATE, OR JULIAN DAY NUMBER. THE DATA WERE DERIVED AT ONE POINT ("OPPSALFJELLET") FROM THE SENORGE.NO INTERNET SITE, WHERE WEATHER DATA ARE INTERPOLATED INTO A HIGH-RESOLUTION GRID ALL OVER NORWAY. THE DATA WERE DERIVED AS THE 24-h PRECIPITATION SUM, THE 24-h TEMPERATURE MEAN, AND THE 24-h MEAN SNOW DEPTH AT 08:00 ON THE DAY OF ACQUISITION

Seasonal sorting	Acquisition	Date	Season	Daily precipitation mm	Mean daily temp °C	Snow depth cm
1	5	14.02.2013	Winter	1.1	-6.7	77.8
2	3	15.05.2012	Spring	0.3	6.3	0
3	4	03.07.2012	Summer	3.0	13.1	0
4	8	13.07.2011	Summer	1.3	13.0	0
5	1	23.07.2011	Summer	50.1	13.4	0
6	7	24.07.2011	Summer	29.3	15.5	0
7	6	01.09.2011	Autumn	3.0	10.7	0
8	2	05.09.2011	Autumn	19.6	13.4	0

tions 3 and 8 had noisy heights, but still generally similar. The similarity in InSAR heights occurred despite a range in season from middle of May through the summer to early autumn with precipitation ranges from 0 up to 50 mm and temperature variations between 6 °C and 16 °C. This temporal stability of InSAR height is promising for forest monitoring. This finding is also similar to findings with TanDEM-X in a boreal forest in Finland [18].

Acquisition 5 deviated considerably from the other acquisitions. The InSAR heights were much lower, which resulted in the much larger slope in the biomass regression model (see Table III and Fig. 1). Acquisition 5 is a winter acquisition, and the deviation from the other acquisitions is attributable to two effects. First, the deeper penetration can partly be attributed to needle and leaf fall during autumn. Working in coniferous boreal forests, [18] found a gradual 2-m decrease in TanDEM-X InSAR height from the end of the growing season to the late fall, or early winter, and attributed this to needle fall.

Second, the temperatures were well below zero (see Table VI), which would cause a deeper penetration into the forest canopy. The interaction between the microwaves and a forest canopy is influenced by the dielectric properties, which are largely determined by liquid water. The dielectric properties of the vegetation vary with seasonal changes in plant physiology and weather conditions [6], [19]. Liquid water present inside the vegetation tissues or as films on the foliage surfaces from intercepted precipitation or dew will increase the attenuation of the microwaves through the canopy and increase InSAR height. On the contrary, freezing will remove such liquid water and reduce attenuation and InSAR height.

References [20] and [21] fitted spruce biomass models to InSAR heights from the X-band SRTM, which was acquired in February 2000 in Norway. The obtained models had slope parameters of 12–15 t/ha/m, which is similar to what was found for all the nonwinter acquisitions in this study, but very different from the winter acquisition. It is possible that the SRTM acquisitions were obtained during nonfrozen conditions, but this is uncertain due to unstable weather in February 2000. Although below-zero temperatures and dry snow dominated, there were days during the SRTM mission with temperatures around and slightly above zero. For example, on February 13, 2000, there was precipitation partly as moist snow and sleet.

A study from a Siberian boreal forest with phased array type L-band synthetic aperture radar showed that frozen conditions reduced the phase height from 8 to 4 m [7]. This corresponds fairly well to the present results, where InSAR heights decreased from about 9 m with unfrozen conditions to about 5 m under frozen conditions (see Table III). Some differences could be attributed also to differences in wavelength, i.e., X-band versus L-band.

IV. CONCLUSION

Altogether, the results have demonstrated that forest monitoring based on InSAR height from regularly repeated data takes is a promising method. This is particularly the case if the technical properties and the season of the acquisitions are kept constant. However, both the technical properties and the weather conditions could be allowed to vary within certain ranges with only minor effects on the InSAR heights. Single co-pol acquisitions should be preferred; as should baseline values around 200–400 m corresponding to HoA values around 20–50 m. One should use either unfrozen or frozen conditions. For other forest types and forests growing in another climate, other considerations should be taken linked to dry seasons and annual leaf fall.

ACKNOWLEDGMENT

The authors would like to thank the German Aerospace Center (DLR) for providing the TanDEM-X data and the forest estate Fritzøe for providing the forest management data.

REFERENCES

[1] R. N. Treuhaft and P. R. Siqueira, "The calculated performance of forest structure and biomass estimates from interferometric radar," *Waves Random Media*, vol. 14, no. 2, pp. S345–S358, Apr. 2004.
[2] S. Solberg, R. Astrup, J. Breidenbach, B. Nilsen, and D. Weydahl, "Monitoring spruce volume and biomass with InSAR data from TanDEM-X," *Remote Sens. Environ.*, vol. 139, pp. 60–67, Dec. 2013.
[3] J. Deutscher, R. Perko, K. Gutjahr, M. Hirschmugl, and M. Schardt, "Mapping tropical rainforest canopy disturbances in 3D by COSMO-SkyMed spotlight InSAR-stereo data to detect areas of forest degradation," *Remote Sens.*, vol. 5, no. 2, pp. 648–663, Feb. 2013.
[4] D. J. Weydahl, J. Sagstuen, O. B. Dick, and H. Ronning, "SRTM DEM accuracy assessment over vegetated areas in Norway," *Int. J. Remote Sens.*, vol. 28, no. 16, pp. 3513–3527, Aug. 2007.
[5] S. Solberg, R. Astrup, and D. J. Weydahl, "Detection of forest clear-cuts with Shuttle Radar Topography Mission (SRTM) and tandem-X InSAR data," *Remote Sens.*, vol. 5, no. 11, pp. 5449–5462, Oct. 2013.
[6] J. Way *et al.*, "The effect of changing environmental-conditions on microwave signatures of forest ecosystems—Preliminary-results of the March 1988 Alaskan aircraft SAR experiment," *Int. J. Remote Sens.*, vol. 11, no. 7, pp. 1119–1144, Jul. 1990.

DOI til publisert versjon / DOI to published version: 10.1109/TGRS.2014.2346473

[7] C. Thiel and C. Schmullius, “Investigating the impact of freezing on the ALOS PALSAR InSAR phase over Siberian forests,” *Remote Sens. Lett.*, vol. 4, no. 9, pp. 900–909, Sep. 2013.

[8] *Landsskogtakseringens Feltinstruks 2008, Håndbok fra Skog og Landskap 05/08*, Anon, Ås, Norway, 2008.

[9] L. G. Marklund, *Biomassafunktioner för tall, gran och björk i Sverige*. Uppsala, Sweden: Sveriges Landbruksuniversitet, 1988, pp. 1–73.

[10] M. Martone *et al.*, “Coherence evaluation of TanDEM-X interferometric data,” *ISPRS J. Photogramm. Remote Sens.*, vol. 73, pp. 21–29, Sep. 2012.

[11] R. M. Goldstein and C. L. Werner, “Radar interferogram filtering for geophysical applications,” *Geophys. Res. Lett.*, vol. 25, no. 21, pp. 4035–4038, Nov. 1998.

[12] J. I. H. Askne, P. B. G. Dammert, L. M. H. Ulander, and G. Smith, “C-band repeat-pass interferometric SAR observations of the forest,” *IEEE Trans. Geosci. Remote Sens.*, vol. 35, no. 1, pp. 25–35, Jan. 1997.

[13] T. Mette, K. P. Papathanassiou, and I. Hajnsek, “Biomass estimation from polarimetric SAR interferometry over heterogeneous forest terrain,” in *Proc. IEEE Int. Geosci. Remote Sens. Symp.*, Anchorage, AK, USA, 2004, pp. 511–514.

[14] I. H. Woodhouse, “Predicting backscatter–biomass and height–biomass trends using a macroecology model,” *IEEE Trans. Geosci. Remote Sens.*, vol. 44, no. 4, pp. 871–877, Apr. 2006.

[15] R. Webster, “Regression and functional relations,” *Eur. J. Soil Sci.*, vol. 48, no. 3, pp. 557–566, Sep. 1997.

[16] T. O. Kvålseth, “Cautionary note about R2,” *Amer. Stat.*, vol. 39, no. 4, pp. 279–285, Nov. 1985.

[17] O. Schabenberger and F. J. Pierce, *Contemporary Statistical Models for the Plant & Soil Sciences*. Boca Raton, FL, USA: CRC Press, 2001.

[18] J. Praks, C. Demirpolat, O. Antropov, and M. Hallikainen, “On forest height retrieval from spaceborne X-band inferometric SAR images under variable seasonal conditions,” in *Proc. XXXII Finnish URSI Conv. Radio Sci. SMARAD Semin.*, Otaniemi, Finland, Apr. 24–25, 2013, pp. 115–118.

[19] K. Sarabandi, “ Δk-radar equivalent of interferometric SAR’s: A theoretical study for determination of vegetation height,” *IEEE Trans. Geosci. Remote Sens.*, vol. 35, no. 5, pp. 1267–1276, Sep. 1997.

[20] S. Solberg, R. Astrup, O. M. Bollandsas, E. Naesset, and D. J. Weydahl, “Deriving forest monitoring variables from X-band InSAR SRTM height,” *Can. J. Remote Sens.*, vol. 36, no. 1, pp. 68–79, Feb. 2010.

[21] S. Solberg *et al.*, “Estimating spruce and pine biomass with interferometric X-band SAR,” *Remote Sens. Environ.*, vol. 114, no. 10, pp. 2353–2360, Oct. 2010.

Svein Solberg (M’13) received the M.Sc. degree in forestry in 1985 and the Dr.Agric. degree on forest health monitoring in 1999.

Since 1990, he has been a Researcher with the Norwegian Forest and Landscape Institute, Ås, Norway. During 2008–2013, he had a professorship in environmental monitoring with the University of Life Sciences, Ås. He has worked on a variety of remote sensing technologies and has developed methods for deriving leaf area index and single-tree segmentation from airborne laser scanning. In recent years, he has focused on SAR and, in particular, interferometric X-band SAR and radargrammetry for monitoring of volume and biomass, as well as detection of logging and storm damage. He has authored or coauthored 43 papers published in international peer-reviewed journals. His major field of research is on monitoring forest disturbance and resources, partly based on remote sensing methods.

Dan Johan Weydahl received the B.Sc. degree in electronic communication and the Dipl.Eng. degree from the University of Salford, Salford, U.K., in 1988 and 1991, respectively, and the Ph.D. degree from the University of Oslo, Oslo, Norway, in 1998.

Since 1989, he has been a Scientist with the Norwegian Defence Research Establishment, Kjeller, Norway. He has contributed to several international scientific work packages organized through Western European Armament Group European Cooperative Long-Term Initiative for Defense, participated in the European Multisensor Airborne Campaign, been a Coinvestigator of an ESA AO-TanDEM project, and been the Principal Investigator for an X-SAR/SRTM project. He is currently the Principal Investigator for Envisat ASAR, ALOS PALSAR, TerraSAR-X, and RADARSAT-2. He also gives lectures in synthetic aperture radar (SAR) image analysis at the University of Oslo. His research interests are in satellite image processing, SAR image calibration, multitemporal SAR image change detection and analysis, and SAR interferometry and polarimetry.

Rasmus Astrup received the Ph.D. degree in forest science from The University of British Columbia, Vancouver, Canada.

He is currently the Director for the Department of Forest Resources with the Norwegian Forest and Landscape Institute, Ås, Norway. His research interests include forest inventory and forest modeling with focus on the interface between forest and climate change. In forest inventory, his main research interest is the development of inventory methods that combine remote sensing with field-based inventories. In forest modeling, his main interest is the development of simulation models for the prediction of national and regional forest development.